









Outage Analysis of TAS-NOMA Systems With Multi-Antenna Users Over α - μ Fading

Fernando D. Almeida García ^{*}, Maria C. Luna Alvarado [†], Lenin P. Jiménez Jiménez [†],
Gustavo Fraidenraich [†], Michel D. Yacoub [†], Nathaly V. Orozco Garzón [‡],
José D. Vega-Sánchez [§], and Henry R. Carvajal Mora [§]

Wireless and Artificial Intelligence (WAI) Laboratory, National Institute of Telecommunications (INATEL)^{*}

School of Electrical and Computer Engineering, University of Campinas (UNICAMP)[†]

Faculty of Engineering and Applied Sciences (FICA), Universidad de Las Américas (UDLA)[‡]

Colegio de Ciencias e Ingenierías "El Politécnico", Universidad San Francisco de Quito (USFQ)[§]

Email: fernando.almeida@inatel.br^{*}

Abstract—This paper analyzes the outage performance of downlink NOMA systems with transmit antenna selection (TAS) and multi-antenna users over α - μ fading. Maximal-ratio combining (MRC) and equal-gain combining (EGC) are considered, with imperfect successive interference cancellation (ipSIC) explicitly modeled. Exact closed-form outage probability (OP) expressions and asymptotic results are derived, offering insights into diversity and coding gains. Simulations validate the analysis, showing that TAS improves the far user's performance and that MRC outperforms EGC. The results also quantify the loss from ipSIC, and highlight the impact of power allocation on joint OP. The proposed framework serves as a unified tool for evaluating TAS-NOMA systems under generalized fading, providing design insights for B5G/6G networks.

Keywords—Non-orthogonal multiple access, transmit antenna selection, maximal-ratio combining, equal-gain combining, α - μ fading, imperfect successive interference cancellation.

I. Introduction

Non-orthogonal multiple access (NOMA) has emerged as a key enabling technology for fifth-generation (5G) and beyond (B5G) mobile networks, allowing multiple mobile terminals to communicate simultaneously with a base station (BS) over the same radio resource. NOMA can be implemented through code-domain schemes, alternative waveforms, or power-domain allocation. In the latter, successive interference cancellation (SIC) is employed at the receivers; however, practical limitations result in residual interference, which degrades system performance.

The performance of NOMA systems—characterized in terms of outage probability (OP)—has been extensively studied under diverse transmission schemes (e.g., downlink, uplink, cooperative), fading environments (e.g., Rayleigh, Weibull, Nakagami- m , mixture

of Gamma (MoG), κ - μ , α - μ , etc.), diversity techniques at the transmitter (e.g., transmit antenna selection (TAS), beamforming (BF)) and receiver (e.g., maximal-ratio combining (MRC), equal-gain combining (EGC)), and under both perfect and imperfect SIC (ipSIC). A summary of representative contributions is provided in Table I, which also indicates the nature of the OP results, i.e., whether exact, approximate, asymptotic, or not derived.

As summarized in Table I, NOMA is often combined with multi-antenna transmission (e.g., TAS) and reception diversity (e.g., MRC, EGC) to improve spectral efficiency and reliability. However, the impact of ipSIC has not been thoroughly addressed in the literature, despite its practical relevance. Moreover, recent works have shown that the α - μ distribution provides an accurate characterization of fading at millimeter-wave frequencies [27], [28], making it an attractive model for future wireless systems.

To the best of our knowledge, the challenging joint performance evaluation of TAS with MRC/EGC, and ipSIC over α - μ fading channels has not been conducted. To fill this gap, this work investigates the performance of a multi-antenna downlink NOMA system over α - μ fading with ipSIC. Specifically, we analyze the users' OP and derive *novel exact and asymptotic expressions*. The functional form of the α - μ model allows for the investigation of both MRC and EGC combining schemes with the same level of mathematical involvement. Table I highlights how our work distinguishes itself from those related in the literature.

In the following, $\Pr[\cdot]$ denotes probability; $\mathbb{E}[\cdot]$, expectation; $\mathbb{V}[\cdot]$, variance; $|\cdot|$, absolute value; $\Gamma(\cdot)$, the gamma function; and \simeq , "asymptotically equal to around zero," i.e., $f(x) \simeq g(x) \iff \lim_{x \rightarrow 0} \frac{f(x)}{g(x)} = 1$.

Table I: Comparison with the state-of-the-art studies

Paper	NOMA System	Fading Environment	Transmission Diversity	Reception Diversity	Imperfect SIC	OP Analysis
[1]	Downlink	Rayleigh	TAS	NO	NO	Exact
[2], [3], [4], [5], [6]	Downlink	Rayleigh	BF	NO	NO	NO
[7]	Coop. Downlink	Rayleigh	TAS	NO	YES	Exact/Asymptotic
[8]	Coop. Downlink	Rayleigh	TAS	NO	YES	NO
[9]	Downlink	Weibull	TAS	EGC	NO	Exact/Asymptotic
[10]	Downlink	Nakagami- m	NO	NO	YES	NO
[11]	Downlink	Nakagami- m	NO	NO	YES	Exact/Asymptotic
[12]	Downlink	Nakagami- m	TAS	MRC	NO	Exact
[13]	Coop. Downlink	Nakagami- m	TAS	MRC	NO	Exact/Asymptotic
[14]	Uplink	MoG (approx.)	NO	NO	YES	Approximated/Asymptotic
[15]	Uplink/Downlink	MoG (approx.)	NO	NO	NO	Approximated/Asymptotic
[16]	Downlink	Double Rayleigh	NO	NO	NO	Exact
[17]	Downlink	Double Nakagami- m	TAS	NO	NO	Exact/Asymptotic
[18],[19]	Downlink	Shadowed-Rician	TAS	NO	YES	Exact/Asymptotic
[20]	Downlink	κ - μ Shadowed	NO	NO	NO	Exact
[21]	Downlink	η - μ and κ - μ	NO	NO	NO	Exact
[22]	Downlink	κ - μ	NO	NO	YES	NO
[23]	Downlink	α - μ	NO	NO	NO	NO
[24]	Coop. Downlink	α - μ	NO	NO	YES	Exact/Asymptotic
[25]	Downlink	α - μ	NO	NO	YES	Exact and asymptotic
[26]	Downlink	α - μ	NO	NO	NO	Exact
This paper	Downlink	α - μ	TAS	EGC/MRC	YES	Exact and asymptotic

II. System Model

Consider a downlink NOMA system with three nodes: a BS equipped with A transmitting antennas and two users equipped with N receiving antennas. The nearest user is denoted as U_1 and is separated from the BS by a distance of d_1 , whereas the farthest user is denoted as U_2 and is separated from the BS by a distance of d_2 . Let $h_{k,n,a}$ denote the complex channel coefficient between the a -th transmit antenna and the n -th receive antenna of the k -th user, where $k \in \{1, 2\}$. Also, we assume that (i) each fading envelope (i.e., $|h_{k,n,a}|$) follows an α - μ distribution, and (ii) all the channels experience i.i.d. fading, i.e., $|h_{k,n,a}|$ is independent of $|h_{l,p,b}| \forall (k \neq l, n \neq p, a \neq b)$. The probability density function (PDF) of $|h_{k,n,a}|$ is given by [29]

$$f_{|h_{k,n,a}|}(h) = \frac{(\alpha\mu^\mu h^{\alpha\mu-1})}{\Gamma(\mu)\hat{h}^{\alpha\mu}} \exp\left(-\mu\left(\frac{h}{\hat{h}}\right)^\alpha\right), \quad (1)$$

where $\alpha > 0$ is a nonlinearity parameter, $\hat{h} \triangleq \sqrt[\alpha]{\mathbb{E}[|h_{k,n,a}|^\alpha]}$ is the α -root mean value, and $\mu > 0$ is the inverse of the normalized variance of $|h_{k,n,a}|^\alpha$, i.e., $\mu = \mathbb{E}^2[|h_{k,n,a}|^\alpha] / \mathbb{V}[|h_{k,n,a}|^\alpha]$.

A. Transmission and Reception Criteria

Without loss of generality, we assume that the farthest user U_2 experiences poorer channel conditions, i.e., $|h_{1,n,a}|^2 > |h_{2,n,a}|^2$. Accordingly, the BS selects the transmitting antenna that maximizes the signal-

to-interference-plus-noise ratio (SINR) of U_2 .¹ Once the transmitting antenna has been selected, the BS simultaneously sends the information to both users in the same radio resource (time-frequency), resulting in the overlapping of the signals. At the receiver side, the multi-antenna users apply either EGC or MRC to combine the received signal replicas. Accordingly, the BS selects the transmit antenna that provides the best performance, denoted by a^* , based on the following criterion:

$$a^* = \arg \max_{1 \leq a \leq A} \left(\sum_{n=1}^N |h_{2,n,a}|^{\vartheta_\nu} \right)^{2/\vartheta_\nu}, \quad (2)$$

where the index $\nu \in \{\text{EGC}, \text{MRC}\}$ specifies the diversity combining scheme, with $\vartheta_{\text{EGC}} = 1$ and $\vartheta_{\text{MRC}} = 2$.

On the basis of the NOMA principle, the BS sends the superposed signals to both users. Hence, the received signals at the n th antenna of the k th user can be written respectively as

$$y_{k,n} = \left(\sqrt{\rho P} s_1 + \sqrt{(1-\rho)P} s_2 \right) h_{k,n,a^*} + w_{k,n}, \quad (3)$$

where ρ is a power allocation coefficient,² P is the total received power, s_k denotes the complex symbol transmitted by the k th user belonging to a constellation

¹It is worth noting that the analytical framework provided herein can also be used if one seeks to maximize the SINR of U_1 .

²As previously stated, the channel condition of U_1 is superior to U_2 , resulting in more power allocated to U_2 according to the NOMA principle, i.e., $0 \leq \rho < 0.5$.

with unitary mean power, h_{k,n,a^*} is the complex channel coefficient satisfying the criterion in (2), and $w_{k,n}$ is the complex additive white Gaussian noise sample with zero mean and variance N_0/T_s affecting the n th branch of the k th user. In addition, N_0 is the unilateral noise power spectral density and T_s is the symbol duration.

B. Imperfect Successive Interference Cancellation

According to the NOMA principle, user U_1 decodes its own signal by first canceling the signal of U_2 using a successive interference cancellation (SIC) detector. However, in practice, the signal of U_2 cannot be completely eliminated. Thus, by considering the NOMA system model used in [30], [31], where ipSIC is considered, the resulting signal at the n th antenna of U_1 can be written as [30]

$$y_{1,n} = \left(\sqrt{\rho P} s_1 + \xi \sqrt{(1-\rho) P} s_2 \right) h_{1,n,a^*} + w_{1,n}, \quad (4)$$

where $\xi \in \{0, 1\}$ denotes the SIC imperfection level at the receiver of U_1 . In particular, $\xi = 0$ represents perfect SIC (i.e., no residual interference), and $\xi = 1$ represents ipSIC. On the other hand, U_2 decodes its signal directly, that is, without using SIC, because the interference inflicted by U_1 is small and can be considered as noise [30].

C. Signal-to-Interference-Plus-Noise Ratio

At the receiver of U_1 , the combined signal of U_1 and U_2 is detected. Then, according to the adopted system model, the SINR of U_1 is given by $\gamma_{U_1} = \rho/(\xi^2(1-\rho) + 1/\Phi_1)$, where

$$\Phi_1 = \frac{E_s g_\nu}{N_0} \left[\sum_{n=1}^N |h_{1,n,a^*}|^{\vartheta_\nu} \right]^{2/\vartheta_\nu}, \quad (5)$$

$E_s = PT_s$ is the average energy per symbol, E_s/N_0 is the received signal-to-noise ratio (SNR) per symbol, and $\{|h_{1,n,a^*}|\}_{n=1}^N$ is the set of i.i.d. α - μ fading envelopes between the transmitting antenna a^* and the n th receiving antenna of U_1 satisfying the criterion in (2). Furthermore, $g_{\text{EGC}} = 1/N$ and $g_{\text{MRC}} = 1$.

At U_2 , its signal is decoded directly by regarding U_1 's signal as interference. Thus, the SINR of U_2 is given by $\gamma_{U_2} = (1-\rho)/(\rho + 1/\Phi_2)$, where

$$\Phi_2 = \frac{E_s g_\nu}{N_0} \left[\sum_{n=1}^N |h_{2,n,a^*}|^{\vartheta_\nu} \right]^{2/\vartheta_\nu}, \quad (6)$$

and $\{|h_{2,n,a^*}|\}_{n=1}^N$ is the set of i.i.d. α - μ fading envelopes between the transmitting antenna a^* and the n th receiving antenna of U_2 satisfying the criterion in (2).

III. Outage Analysis

In this section, we investigate the performance of a downlink TAS-NOMA system with multi-antenna users over α - μ fading channels. To do so, we begin by characterizing Φ_1 and Φ_2 .

Recalling that $|h_{1,n,a^*}|$ and $|h_{2,n,a^*}|$ are independent fading envelopes, and since TAS is applied to maximize the SINR of U_2 , the choice of the transmitting antenna a^* is independent of U_1 [19], [17] and (by extension) is also independent of Φ_1 . To characterize the PDF of Φ_1 , in an exact manner, we employ the formulation in [32] for the sum of i.i.d. α - μ random variables. By invoking [32, eq. (17)] and applying successive variable transformations, the PDF of Φ_1 is obtained as

$$f_{\Phi_1}(\phi_1) = \frac{\vartheta_\nu \beta_\nu}{2K_\nu} \sum_{i=0}^{\infty} \frac{c_i \left(\frac{\phi_1}{K_\nu} \right)^{\frac{\alpha(i+N\mu)}{2} - 1}}{\Gamma\left(\frac{\alpha(i+N\mu)}{\vartheta_\nu}\right)}, \quad (7)$$

where $K_\nu = E_s g_\nu / N_0$, $\beta_\nu = \left(\frac{\alpha \mu^\mu}{\Gamma(\mu) \vartheta_\nu \hat{h}^{\alpha\mu}} \right)^N$, and c_i is given in [32, eq. (6)] under the substitutions $\alpha \mapsto \alpha/\vartheta_\nu$ and $\hat{h} \mapsto \hat{h}^{\vartheta_\nu}$. By integrating (7) with respect to ϕ_1 over the range $0 \leq \phi \leq \phi_1$, the CDF of Φ_1 can be expressed as

$$F_{\Phi_1}(\phi_1) = \beta_\nu \sum_{i=0}^{\infty} \frac{c_i}{\Gamma\left(\frac{\alpha(i+N\mu)}{\vartheta_\nu} + 1\right)} \left(\frac{\phi_1}{K_\nu} \right)^{\frac{\alpha(i+N\mu)}{2}}. \quad (8)$$

On the other hand, according to (2), the choice of the transmitting antenna a^* depends on the statistics of U_2 . In this case, the CDF of Φ_2 can be calculated as

$$\begin{aligned} F_{\Phi_2}(\phi_2) &= \Pr \left[\frac{E_s}{NN_0} \left[\sum_{n=1}^N |h_{2,n,a^*}|^{\vartheta_\nu} \right]^{\frac{2}{\vartheta_\nu}} \leq \phi_2 \right] \\ &= \Pr \left[\left[\sum_{n=1}^N |h_{2,n,1}|^{\vartheta_\nu} \right]^{\frac{2}{\vartheta_\nu}} \leq \delta, \dots, \left[\sum_{n=1}^N |h_{2,n,A}|^{\vartheta_\nu} \right]^{\frac{2}{\vartheta_\nu}} \leq \delta \right], \end{aligned} \quad (9)$$

where $\delta = (\phi_2 NN_0)/E_s$. Taking into account that $|h_{2,n,a}|$ and $|h_{2,p,b}|$, $\forall (n \neq p, a \neq b)$, are i.i.d. fading envelopes, (9) reduces to

$$F_{\Phi_2}(\phi_2) = \left\{ \Pr \left[\frac{E_s g_\nu}{N_0} \left[\sum_{n=1}^N |h_{2,n,a}|^{\vartheta_\nu} \right]^{\frac{2}{\vartheta_\nu}} \leq \phi_2 \right] \right\}^A \quad (10)$$

Leveraging [32, eq. (17)] and following a procedure analogous to that used for deriving (8), the CDF in (10) can be expressed as

$$F_{\Phi_2}(\phi_2) = \beta_\nu^A \sum_{i=0}^{\infty} \left[\eta_{i,\nu} \left(\frac{\phi_2}{K_\nu} \right)^{\frac{\alpha(i+N\mu)}{2}} \right]^A, \quad (11)$$

where $\eta_{i,\nu} = c_i/\Gamma\left(\frac{\alpha(i+N\mu)}{\vartheta_\nu} + 1\right)$. Now, from (11), we let $\left[\sum_{i=0}^{\infty} \eta_{i,\nu} \left(\frac{\phi_2}{K_\nu}\right)^{\frac{\alpha i}{2}}\right]^A = \sum_{i=0}^{\infty} \varrho_{i,\nu} \left(\frac{\phi_2}{K_\nu}\right)^{\frac{\alpha i}{2}}$, where the coefficients $\varrho_{i,\nu}$ are determined after differentiating both sides with respect to $\left(\frac{\phi_2}{K_\nu}\right)^{\alpha/2}$, following the approach in [33]. Thus, after extensive algebraic manipulations, the coefficients $\varrho_{i,\nu}$ can be recursively obtained as

$$\varrho_{0,\nu} = \frac{c_0^A}{\Gamma\left(\frac{N\mu\alpha}{\vartheta_\nu} + 1\right)^A} \quad (12)$$

$$\varrho_{i,\nu} = \frac{\Gamma\left(\frac{N\mu\alpha}{\vartheta_\nu} + 1\right)}{i c_0} \sum_{k=1}^i \frac{(kA - i + k) c_k \varrho_{i-k}}{\Gamma\left(\frac{k\alpha + N\mu\alpha}{\vartheta_\nu} + 1\right)}, \quad i \geq 0. \quad (13)$$

Finally, replacing (12) and (13) into (11), the CDF of Φ_2 can be obtained as

$$F_{\Phi_2}(\phi_2) = \beta_\nu^A \sum_{i=0}^{\infty} \varrho_{i,\nu} \left(\frac{\phi_2}{K_\nu}\right)^{\frac{\alpha}{2}(i+\mu AN)}. \quad (14)$$

The PDF of Φ_2 can be obtained by differentiating (14) with respect to ϕ_2 , yielding

$$f_{\Phi_2}(\phi_2) = \frac{\alpha \beta_\nu^A}{2K_\nu} \sum_{i=0}^{\infty} \varrho_{i,\nu} (i + \mu AN) \left(\frac{\phi_2}{K_\nu}\right)^{\frac{\alpha}{2}(i+\mu AN)-1}. \quad (15)$$

Due to the versatility of the α - μ distribution, the PDF and CDF in (15) and (14) can also model scenarios in which multi-antenna systems operate under i.i.d. Rayleigh [34], Nakagami- m [12], or Weibull [35] fading environments. Now, we proceed to derive the OP of each user, as well as the OP of the overall system.

A. Outage Probability at U_1

The OP of U_1 is defined as the probability that the instantaneous SINR falls below a fixed data rate \tilde{R}_{U_1} , i.e., $P_{\text{out}}^{U_1} \triangleq \Pr\left[\gamma_{U_1} \leq \tilde{R}_{U_1}\right] = F_{\Phi_1}\left(\frac{1}{\rho/\tilde{R}_{U_1} - \xi^2(1-\rho)}\right)$. Thus, after using (8), we obtain

$$P_{\text{out}}^{U_1} = \beta_\nu \sum_{i=0}^{\infty} \frac{c_i \left(K_\nu(\rho/\tilde{R}_{U_1} - \xi^2(1-\rho))\right)^{-\frac{\alpha(i+N\mu)}{2}}}{\Gamma\left(\frac{\alpha(i+N\mu)}{\vartheta_\nu} + 1\right)}. \quad (16)$$

The asymptotic OP is useful to address the system performance at high-SNR regime, i.e., when $E_s/N_0 \rightarrow \infty$. This is the region where reliable communication systems commonly operate. To obtain the asymptotic OP of U_1 , we can use the first term of the series in (16), yielding

$$P_{\text{out}}^{U_1} \simeq P_{\text{out},\infty}^{U_1} = \left(O_{c,1} \frac{E_s}{N_0}\right)^{-O_{d,1}}, \quad (17)$$

where $O_{d,1} = \alpha\mu N/2$ is the diversity gain and

$$O_{c,1} = g_\nu \left(\frac{\rho}{\tilde{R}_{U_1}} - \xi^2(1-\rho)\right) \left(\frac{c_0 \beta_\nu}{\Gamma\left(\frac{N\mu\alpha}{\vartheta_\nu} + 1\right)}\right)^{-\frac{1}{O_{d,1}}} \quad (18)$$

is the coding gain for U_1 .

B. Outage Probability at U_2

Similar to user U_1 , the OP of user U_2 can be obtained as $P_{\text{out}}^{U_2} \triangleq \Pr\left[\gamma_{U_2} \leq \tilde{R}_{U_2}\right] = F_{\Phi_2}\left(\frac{1}{(1-\rho)/\tilde{R}_{U_2} - \rho}\right)$. Thus, using (15), we have

$$P_{\text{out}}^{U_2} = \beta_\nu^A \sum_{i=0}^{\infty} \varrho_{i,\nu} \left(K_\nu \left(\frac{1-\rho}{\tilde{R}_{U_2}} - \rho\right)\right)^{-\frac{\alpha}{2}(i+\mu AN)}, \quad (19)$$

where \tilde{R}_{U_2} is the targeted data rate of U_2 . Further, the asymptotic OP of U_2 can be found as

$$P_{\text{out}}^{U_2} \simeq P_{\text{out},\infty}^{U_2} = \left(O_{c,2} \frac{E_s}{N_0}\right)^{-O_{d,2}}, \quad (20)$$

where $O_{d,2} = \alpha\mu AN/2$ is the diversity gain and

$$O_{c,2} = g_\nu \left(\frac{1-\rho}{\tilde{R}_{U_2}} - \rho\right) \left(\frac{c_0^A \beta_\nu^A}{\Gamma\left(\frac{N\mu\alpha}{\vartheta_\nu} + 1\right)^A}\right)^{-\frac{1}{O_{d,2}}} \quad (21)$$

is the coding gain for U_2 . Notice from (17) and (20) that the diversity gains of both users depend on the fading parameters (α and μ) and the number of receiving antennas (N), whereas the diversity gain of U_2 takes also into account the number of transmitting antennas (A), delivering additional diversity to the user with worst channel conditions. This additional gain allows us to reduce the allocated power for the second (farthest) user, thus improving the overall system performance.

C. Overall Outage Probability

For the TAS-NOMA system under consideration, the overall OP is defined as the probability that an outage event occurs at either U_1 or U_2 , and is given by

$$P_{\text{out}}^{\text{overall}} = \Pr\left[\gamma_{U_1} \leq \tilde{R}_{U_1}, \gamma_{U_2} \leq \tilde{R}_{U_2}\right]. \quad (22)$$

From (16) and (19), and since γ_{U_1} and γ_{U_2} are statistically independent, we can finally rewrite (22) as

$$P_{\text{out}}^{\text{overall}} = 1 - (1 - P_{\text{out}}^{U_1})(1 - P_{\text{out}}^{U_2}). \quad (23)$$

From (17) and (20), an asymptotic closed-form expression for the overall OP can be derived as

$$P_{\text{out}}^{\text{overall}} \simeq P_{\text{out},\infty}^{\text{overall}} = 1 - (1 - P_{\text{out},\infty}^{U_1})(1 - P_{\text{out},\infty}^{U_2}). \quad (24)$$

IV. Sample Results and Discussions

This section validates the analytical findings through Monte Carlo simulations. For all figures, the series expansions of $P_{\text{out}}^{U_1}$ and $P_{\text{out}}^{U_2}$ were computed with 200 terms in their respective series.

Fig. 1 shows the overall OP versus E_s/N_0 for different values of N . As expected, performance improves with the number of receive branches. A pronounced gain is observed when N increases from 2 to 4, while the improvements gradually taper off as N increases

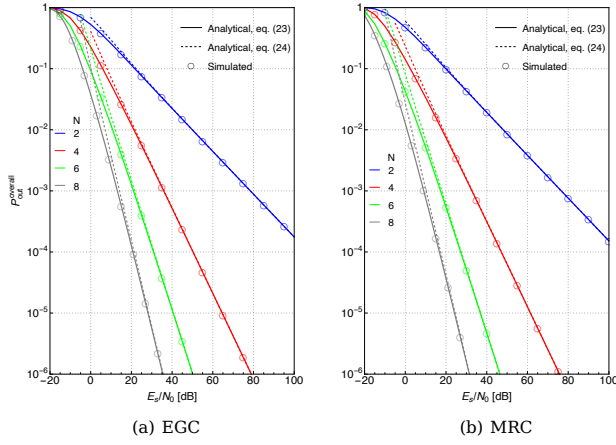


Figure 1: Overall OP versus E_s/N_0 assuming $\alpha = 0.7$, $\mu = 0.5$, $A = 2$, $\hat{h} = 2$, $\xi = 1$, $\rho = 0.5$, $\hat{R}_{U_1} = \hat{R}_{U_2} = 0.5$, and different values of N .

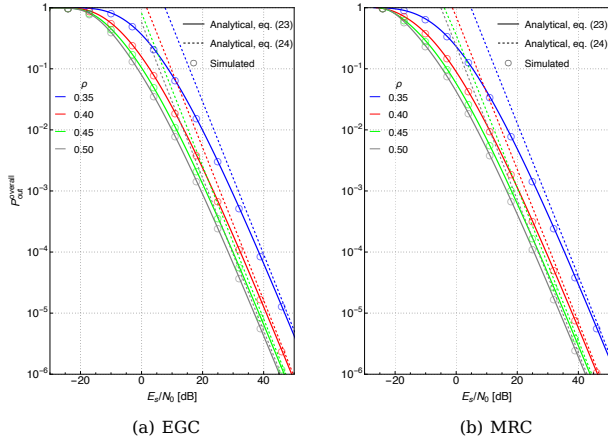


Figure 2: Overall OP versus E_s/N_0 assuming $\alpha = 0.5$, $\mu = 1$, $N = 5$, $A = 3$, $\hat{h} = 2$, $\xi = 1$, $\hat{R}_{U_1} = \hat{R}_{U_2} = 0.5$, and various values of ρ .

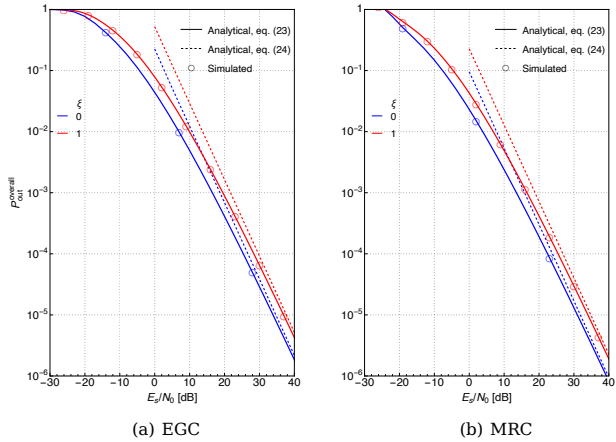


Figure 3: Overall OP versus E_s/N_0 assuming $\alpha = 0.5$, $\mu = 1$, $N = 5$, $A = 7$, $\hat{h} = 2$, $\hat{R}_{U_1} = \hat{R}_{U_2} = 0.5$, and perfect ($\xi = 0$) and imperfect ($\xi = 1$) SIC.

beyond 4, up to 8, with MRC consistently outperforming EGC, as expected. Furthermore, the asymptotic

curves derived in Section III align perfectly with the Monte Carlo results in the high-SNR regime. Fig. 2 illustrates the overall OP versus E_s/N_0 for different power allocation coefficients ρ . A trend similar to Fig. 1 is observed, where increasing ρ lowers the overall OP. This occurs because allocating more power to U_1 reduces its OP, while TAS concurrently improves the performance of U_2 , yielding a net reduction in the system's overall OP. Once again, MRC achieves a slight but consistent gain over EGC, and the asymptotic curves align perfectly with the Monte Carlo simulations in the high-SNR region. Finally, Fig. 3 presents the overall OP versus E_s/N_0 under perfect ($\xi = 0$) and imperfect ($\xi = 1$) SIC. As expected, ipSIC leads to a clear performance degradation, yielding a higher OP for any given E_s/N_0 . This gap remains evident across both the mid- and high-SNR regimes. Consistently, MRC outperforms EGC, while the asymptotic curves closely match the Monte Carlo simulations in the high-SNR region.

V. Conclusions

This work analyzed the outage performance of TAS-NOMA systems with multi-antenna users over α - μ fading channels, considering MRC/EGC combining and the effect of ipSIC. Exact and asymptotic expressions were derived, highlighting diversity and coding gains. Results showed that adding receive antennas improves performance significantly up to four branches, with diminishing returns thereafter. Power allocation strongly impacts joint outage performance, benefiting the near user, while TAS enhances the far user. ipSIC consistently degrades performance, and MRC slightly outperforms EGC. The α - μ model enables a unified treatment of MRC and EGC while capturing realistic fading conditions.

Acknowledgement

This work was funded by the Brasil 6G Project with support from RNP/MCTI (Grant 01245.010604/2020-14), and by the xGMobile Project (Code XGM-AFCCT-2025-8-1-1) with resources from EMBRAPII/MCTI (Grant 052/2023 PPI IoT/Manufatura 4.0) and FAPEMIG Grant PPE-00124-23. The work of M. C. L. Alvarado was supported by the São Paulo Research Foundation (FAPESP) under Grant 2023/02578-1. The work of L. P. J. Jiménez, G. Fraidenraich and M. D. Yacoub were supported by the Conselho Nacional de Desenvolvimento Científico e Tecnológico (CNPq) under Grants 141108/2023-1, 302077/2022-7 and 305038/2024-9. This work was also supported in part by the Universidad San Francisco de Quito (USFQ) through the Poli-Grants Program under Grant 33595.

References

- [1] D.-T. Do, T.-L. Nguyen, and B. M. Lee, "Transmit antenna selection schemes for NOMA with randomly moving interferers in interference-limited environment," *Electronics*, vol. 9, no. 1, pp. 1–15, Jan. 2020.
- [2] Q. Zhang, Q. Li, and J. Qin, "Robust beamforming for nonorthogonal multiple-access systems in MISO channels," *IEEE Trans. Veh. Technol.*, vol. 65, no. 12, pp. 10231–10236, Dec. 2016.
- [3] F. Zhu, Z. Lu, J. Zhu, J. Wang, and Y. Huang, "Beamforming design for downlink non-orthogonal multiple access systems," *IEEE Access*, vol. 6, pp. 10956–10965, Jan. 2018.
- [4] X. Chen, Z. Zhang, C. Zhong, and D. W. K. Ng, "Exploiting multiple-antenna techniques for non-orthogonal multiple access," *IEEE J. Sel. Areas Commun.*, vol. 35, no. 10, pp. 2207–2220, Jul. 2017.
- [5] F. Alavi, K. Cumanan, Z. Ding, and A. G. Burr, "Robust beamforming techniques for non-orthogonal multiple access systems with bounded channel uncertainties," *IEEE Commun. Lett.*, vol. 21, no. 9, pp. 2033–2036, Sep. 2017.
- [6] H. M. Al-Obiedollah, K. Cumanan, J. Thiagalingam, A. G. Burr, Z. Ding, and O. A. Dobre, "Energy efficient beamforming design for MISO non-orthogonal multiple access systems," *IEEE Trans. Commun.*, vol. 67, no. 6, pp. 4117–4131, Jun. 2019.
- [7] Z. Mobini, M. Mohammadi, T. A. Tsiftsis, Z. Ding, and C. Tellambura, "New antenna selection schemes for full-duplex cooperative MIMO-NOMA systems," *IEEE Trans. Commun.*, vol. 70, no. 7, pp. 4343–4358, Jul. 2022.
- [8] X. Pei, H. Yu, M. Wen, Q. Li, and Z. Ding, "Secure outage analysis for cooperative NOMA systems with antenna selection," *IEEE Trans. Veh. Technol.*, vol. 69, no. 4, pp. 4503–4507, Apr. 2020.
- [9] L. P. J. Jiménez, F. D. A. García, M. C. L. Alvarado, G. Fraidenraich, M. D. Yacoub, J. C. S. S. Filho, and E. R. De Lima, "Performance analysis of downlink MIMO-NOMA systems over Weibull fading channels," in *IEEE Globecom Workshops (GC Wkshps)*, Rio de Janeiro, Brazil, Dec. 2022, pp. 729–734.
- [10] L. Bariah, S. Muhaidat, and A. Al-Dweik, "Error probability analysis of non-orthogonal multiple access over Nakagami- m fading channels," *IEEE Trans. Commun.*, vol. 67, no. 2, pp. 1586–1599, Feb. 2019.
- [11] T. Hou, X. Sun, and Z. Song, "Outage performance for non-orthogonal multiple access with fixed power allocation over Nakagami- m fading channels," *IEEE Commun. Lett.*, vol. 22, no. 4, pp. 744–747, Apr. 2018.
- [12] Y. Zhang, J. Ge, and E. Serpedin, "Performance analysis of nonorthogonal multiple access for downlink networks with antenna selection over Nakagami- m fading channels," *IEEE Trans. Veh. Technol.*, vol. 66, no. 11, pp. 10590–10594, Nov. 2017.
- [13] M. Aldababsa, E. Güven, M. A. Durmaz, C. Göztepe, G. K. Kurt, and O. Kucur, "Unified performance analysis of antenna selection schemes for cooperative MIMO-NOMA with practical impairments," *IEEE Trans. Wireless Commun.*, vol. 21, no. 6, pp. 4364–4378, 2022.
- [14] N. P. Le, L. C. Tran, X. Huang, J. Choi, E. Dutkiewicz, S. L. Phung, and A. Bouzerdoum, "Performance analysis of uplink NOMA systems with hardware impairments and delay constraints over composite fading channels," *IEEE Trans. Veh. Technol.*, vol. 70, no. 7, pp. 6881–6897, Jul. 2021.
- [15] A. Agarwal, R. Chaurasiya, S. Rai, and A. K. Jagannatham, "Outage probability analysis for NOMA downlink and uplink communication systems with generalized fading channels," *IEEE Access*, vol. 8, pp. 220461–220481, Dec. 2020.
- [16] N. Jaiswal and N. Purohit, "Performance of downlink NOMA-enabled vehicular communications over double Rayleigh fading channels," *IET Commun.*, vol. 14, pp. 3652–3660, Dec. 2020.
- [17] —, "Performance analysis of NOMA-enabled vehicular communication systems with transmit antenna selection over double Nakagami- m fading," *IEEE Trans. Veh. Technol.*, vol. 70, no. 12, pp. 12725–12741, Dec. 2021.
- [18] X. Yue, Y. Liu, Y. Yao, T. Li, X. Li, R. Liu, and A. Nallanathan, "Outage behaviors of NOMA-based satellite network over shadowed-Rician fading channels," *IEEE Trans. Veh. Technol.*, vol. 69, no. 6, pp. 6818–6821, Jun. 2020.
- [19] H. Shuai, K. Guo, K. An, Y. Huang, and S. Zhu, "Transmit antenna selection in NOMA-based integrated satellite-HAP-terrestrial networks with imperfect CSI and SIC," *IEEE Wireless Commun. Lett.*, vol. 11, no. 8, pp. 1565–1569, Aug. 2022.
- [20] B. M. ElHalawany, F. Jameel, D. B. da Costa, U. S. Dias, and K. Wu, "Performance analysis of downlink NOMA systems over κ - μ shadowed fading channels," *IEEE Trans. Veh. Technol.*, vol. 69, no. 1, pp. 1046–1050, Jan. 2020.
- [21] P. Sharma, A. Kumar, and M. Bansal, "Performance analysis of downlink NOMA over η - μ and κ - μ fading channels," *IET Commun.*, vol. 14, no. 3, pp. 522–531, Dec. 2019.
- [22] A. S. Arias, L. C. Huera, B. S. Rueda, H. R. Carvajal, N. V. Orozco, and F. D. Almeida, "On the secrecy outage probability of NOMA systems affected by imperfect SIC over κ - μ fading channels," *Journal of Communications*, vol. 18, no. 3, pp. 147–155, 2023.
- [23] V. Kumar, B. Cardiff, S. Prakriya, and M. F. Flanagan, "Delay violation probability and effective rate of downlink NOMA over α - μ fading channels," *IEEE Trans. Veh. Technol.*, vol. 69, no. 10, pp. 11241–11252, Oct. 2020.
- [24] X. Li, J. Li, Y. Liu, Z. Ding, and A. Nallanathan, "Residual transceiver hardware impairments on cooperative NOMA networks," *IEEE Trans. Wireless Commun.*, vol. 19, no. 1, pp. 680–695, Jan. 2020.
- [25] S. Arzykulov, G. Nauryzbayev, M. S. Hashmi, A. M. Eltawil, K. M. Rabie, and S. Seilov, "Hardware- and interference-limited cognitive IoT relaying NOMA networks with imperfect SIC over generalized non-homogeneous fading channels," *IEEE Access*, vol. 8, pp. 72942–72956, Apr. 2020.
- [26] A. Alqahtani, E. Alsusa, A. Al-Dweik, and M. Al-Jarrah, "Performance analysis for downlink NOMA over α - μ generalized fading channels," *IEEE Trans. Veh. Technol.*, vol. 70, no. 7, pp. 6814–6825, Jul. 2021.
- [27] T. R. R. Marins, A. A. dos Anjos, V. M. R. Peñarrocha, L. Rubio, J. Reig, R. A. A. de Souza, and M. D. Yacoub, "Fading evaluation in the mm-wave band," *IEEE Trans. Commun.*, vol. 67, no. 12, pp. 8725–8738, Dec. 2019.
- [28] T. R. R. Marins, A. A. D. Anjos, C. R. N. D. Silva, V. M. R. Peñarrocha, L. Rubio, J. Reig, R. A. A. De Souza, and M. D. Yacoub, "Fading evaluation in standardized 5G millimeter-wave band," *IEEE Access*, vol. 9, pp. 67268–67280, Apr. 2021.
- [29] M. D. Yacoub, "The α - μ distribution: A physical fading model for the Stacy distribution," *IEEE Trans. Veh. Technol.*, vol. 56, no. 1, pp. 27–34, Jan. 2007.
- [30] I. Abu Mahady, E. Bedeer, S. Ikki, and H. Yanikomeroglu, "Sum-Rate Maximization of NOMA Systems Under Imperfect Successive Interference Cancellation," *IEEE Commun. Lett.*, vol. 23, no. 3, pp. 474–477, Mar. 2019.
- [31] M. Sfredo, E. M. Garcia Fernandez, and H. R. Carvajal Mora, "Physical Layer Security in Power-Domain NOMA Using Improper Gaussian Signals," in *2021 IEEE 94th Vehicular Technology Conference (VTC2021-Fall)*, 2021, pp. 01–05.
- [32] F. D. A. García, F. R. A. Parente, M. D. Yacoub, and J. C. S. Santos Filho, "On the exact sum PDF and CDF of α - μ variates," *IEEE Trans. Wireless Commun.*, vol. 22, no. 8, pp. 5084–5095, Aug. 2023.
- [33] —, "Exact κ - μ sum statistics," *IEEE Wireless Commun. Lett.*, vol. 12, no. 7, pp. 1284–1288, Jul. 2023.
- [34] F. A. García, H. Carvajal Mora, and N. O. Garzón, "Improved exact evaluation of equal-gain diversity receivers in Rayleigh fading channels," *IEEE Access*, vol. 10, pp. 26974–26984, Mar. 2022.
- [35] F. D. A. García, F. R. A. Parente, G. Fraidenraich, and J. C. S. Santos Filho, "Light exact expressions for the sum of Weibull random variables," *IEEE Wireless Commun. Lett.*, vol. 10, no. 11, pp. 2445–2449, Nov. 2021.